

In-plane vibration analysis of cantilevered circular arc beams undergoing rotational motion

Guang Hui Zhang¹, Zhan Sheng Liu² and Hong Hee Yoo^{3,*}

¹*School of Mechanical Engineering, Hanyang University*

²*School of Energy Science and Engineering, Harbin Institute of Technology, China*

³*School of Mechanical Engineering, Hanyang University*

(Manuscript Received May 8, 2006; Revised September 27, 2007; Accepted September 27, 2007)

Abstract

Equations of motion of cantilevered circular arc beams undergoing rotational motion are derived based on a dynamic modeling method developed in this paper. Kane's method is employed to derive the equations of motion. Different from the classical linear modeling method which employs two cylindrical deformation variables, the present modeling method employs a non-cylindrical variable along with a cylindrical variable to describe the elastic deformation. The derived equations (governing the stretching and the bending motions) are coupled but linear, so they can be directly used for vibration analysis. The coupling effect between the stretching and the bending motions, which could not be considered in the conventional modeling method, is considered in this modeling method. The effects of rotational speed, arc angle, and hub radius ratio on the natural frequencies of the rotating circular arc beam are investigated through numerical analysis.

Keywords: Circular arc beam; In-plane vibration; Rotational motion; Hybrid modeling; Stiffness variation; Dimensionless parameter

1. Introduction

Beam structures can be found in many aerospace and mechanical engineering examples such as spacecraft structures, robots, turbine blades, and helicopter blades. For proper designs of such systems, their modal characteristics such as natural frequencies should be identified accurately and effectively. Although abundant literature for the vibration analysis of rotating beams can be found, only a few are related to curved beams. Compared to the modal characteristics of a straight beam, those of a curved beam clearly show a different tendency that originates from the curvature of the beam. Furthermore, the modal characteristics of a rotating beam are significantly different from those of a non-rotating beam. The stiffness variation of a rotating beam results from the stiffening effect which is induced by the centrifugal inertia

force (due to rotational motion). So the curvature and the rotational speed affect the modal characteristics of the beam simultaneously. Therefore, those two effects should be considered simultaneously to obtain the modal characteristics of the rotating curved beam accurately and effectively.

In the 1920's Southwell and Gough [1] introduced an analytical method to obtain the natural frequencies of a rotating beam. Based on the Rayleigh energy method, they proposed an equation to calculate the natural frequencies of a rotating cantilever beam. To obtain more accurate results, Schilhansl [2] derived a linear partial differential equation which governs the bending vibration of a rotating cantilever beam. Not only the natural frequencies but also the mode shapes could be obtained with the equation. Putter and Manor [3] applied the assumed mode method to obtain the modal characteristics of a rotating beam. More recently, Kane et al. [4] introduced a comprehensive theory to deal with the dynamics of a beam

*Corresponding author. Tel.: +82 2220 0446, Fax.: +82 2293 5070
E-mail address: hhyoo@hanyang.ac.kr
DOI 10.1007/s12206-007-1013-x

attached to a base. A new variable, namely the stretch along the elastic axis, was used to account for the geometric stiffening effect appropriately. Based on the method, the effect of Coriolis coupling on the modal characteristics of a rotating beam was successfully investigated by Yoo and Shin [5].

The out-of-plane and the in-plane motions of a curved beam are coupled in general. However, if the cross section of the curved beam is symmetric and the thickness of the beam is small in comparison with the radius of the beam, the out-of-plane and the in-plane motions can be decoupled [6, 7] without losing modeling integrity. The Rayleigh-Ritz method could be used to obtain the natural frequencies of inextensional [8, 9] and extensional [6, 10] in-plane vibrations of ring segments. Upper and lower bounds for the fundamental frequency of in-plane transverse vibration of a cantilevered curved beam were determined by Laura [11]. Laura derived the fundamental natural frequency equation by means of the Rayleigh-Ritz method. Three curved beam elements were investigated to solve the problem of radial vibrations of curved beams [12].

The purpose of this paper is to develop a modeling method to investigate the modal characteristics of cantilevered circular arc beams undergoing rotational motion. For the modeling method a hybrid set of deformation variables are employed. The use of hybrid deformation variables, which distinguishes the present modeling method from other conventional methods, is the key ingredient to derive accurate linear equations of motion which provide proper motion induced stiffness variations. Moreover, the effect of coupling between the stretching and the bending motion on the modal characteristics can be also considered in the equations. The effects of the curvature along with the hub radius and the rotating speed on the modal characteristics of curved beams are investigated with numerical examples.

2. Equations of motion

2.1 Employed assumption and geometric constraint equation

In this section, equations of motion of a cantilever curved beam undergoing rotational motion are derived based on the following assumptions. The beam has homogeneous and isotropic material properties. The neutral axis and the centroidal axis of the beam cross-section coincide so that the effect of the eccen-

tricity need not be considered. The beam has a slender shape so that the shear effect and the rotary inertia effect can be neglected. These assumptions result in simplified equations of motion with which the main issues of this study (variations of modal characteristics of rotating cantilevered curved beams) can be effectively investigated.

Fig. 1 shows the configuration of a rotating curved beam attached to a rigid hub. A generic point P_0 which lies on the undeformed neutral axis moves to P when the beam is deformed. Cylindrical deformation variables u_r and u_θ are conventionally employed to express the elastic deformation. In the present study, a non-cylindrical variable s denoting the stretch along the neutral axis of the beam is employed instead of u_θ .

There is a geometric relation between the stretch s and the cylindrical deformation variables. This relation is later used to drive the generalized inertia forces. From the differential geometry (see Ref. [14]), the following equation can be obtained.

$$OP = \int_b^{\theta} \left[\left(R + \frac{\partial u_\theta}{\partial \sigma} \right)^2 + \left(\frac{\partial u_r}{\partial \sigma} \right)^2 \right]^{\frac{1}{2}} d\sigma \tag{1}$$

where OP denotes the length of the curved beam segment after deformation. Employing the stretch variable s , the left hand side of Eq. (1) can be expressed as $R\theta + s$. So,

$$R\theta + s = \int_b^{\theta} \left[\left(R + \frac{\partial u_\theta}{\partial \sigma} \right)^2 + \left(\frac{\partial u_r}{\partial \sigma} \right)^2 \right]^{\frac{1}{2}} d\sigma \tag{2}$$

By using binomial expansion of the integrand of Eq. (2), the following approximated equation can

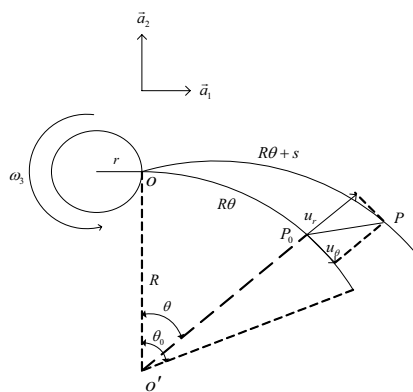


Fig. 1. Configuration of a rotating cantilevered circular arc beam.

be obtained.

$$s = u_\theta + \frac{1}{2R} \int_0^\theta \left(\frac{\partial u_r}{\partial \sigma} \right)^2 d\sigma \quad (3)$$

2.2 Approximation of deformation variables and strain energy expression

In the present work, s and u_r are approximated by using mode functions and the corresponding coordinates to drive the ordinary differential equations of motion. A modeling method employing hybrid deformation variables is described in detail in Ref. [5]. By employing the Rayleigh-Ritz method, the deformation variables are approximated as follows:

$$s = \sum_{i=1}^{\mu_1} \Phi_{1i}(\theta) q_{1i}(t) \quad (4)$$

$$u_r = \sum_{i=1}^{\mu_2} \Phi_{2i}(\theta) q_{2i}(t) \quad (5)$$

where q_{1i} and q_{2i} denote the generalized coordinates;

Φ_{1i} and Φ_{2i} denote the spatial functions of s and u_r ; μ_1 and μ_2 denote the numbers of the spatial function, Employing the stretch variable s , the total strain energy can be expressed as

$$U = \frac{1}{2R} \int_0^{\theta_0} EA \left(\frac{\partial s}{\partial \theta} \right)^2 d\theta + \frac{EI}{2R^3} \int_0^{\theta_0} \left(\frac{\partial^2 u_r}{\partial \theta^2} + u_r \right)^2 d\theta \quad (6)$$

where E denotes Young's modulus, A denotes the cross-section area, I denotes the second area moment of inertia of the cross-section, R denotes the radius of the circular arc, and θ_0 denotes the arc angle.

2.3 Equations of motion

With the assumptions given in Section 2.1, the equations of motion can be derived from the following equation (see Ref. [13]).

$$R \int_0^{\theta_0} \rho \bar{a}^p \cdot \left(\frac{\partial \bar{v}^p}{\partial \dot{q}_i} \right) d\theta + \frac{\partial U}{\partial \dot{q}_i} = 0 \quad (7)$$

where ρ denotes the mass per unit length of the beam and q_i consists of q_{1i} and q_{2i} .

The acceleration \bar{a}^p can be obtained by differentiating the velocity \bar{v}^p with respect to time, which can be obtained by using the following equation.

$$\bar{v}^p = \bar{v}^o + \bar{\omega}^A \times (\bar{r} + \bar{u}) + \frac{d}{dt} (\bar{r} + \bar{u}) \quad (8)$$

where \bar{v}^O denotes velocity of point O fixed to the rigid hub;

$\bar{\omega}^A$ denotes angular velocity of the rigid hub; \bar{r} denotes the position vector of the generic point; \bar{u} denotes the elastic deformation vector, and the third term in the above denotes the time differentiation of vector $\bar{r} + \bar{u}$ in the frame A . Using the coordinate system fixed to the rigid hub, \bar{v}^O , $\bar{\omega}^A$, \bar{r} and \bar{u} can be expressed as follows:

$$\bar{v}^O = \omega_3 r \bar{a}_2 \quad (9)$$

$$\bar{\omega}^A = \omega_3 \bar{a}_3 \quad (10)$$

$$\bar{r} = R \sin \theta \bar{a}_1 - R(1 - \cos \theta) \bar{a}_2 \quad (11)$$

$$\bar{u} = u_r (\cos \theta \bar{a}_2 + \sin \theta \bar{a}_1) + u_\theta (\cos \theta \bar{a}_1 - \sin \theta \bar{a}_2) \quad (12)$$

The velocity of point P can be obtained as follows:

$$\begin{aligned} \bar{v}^p = & \left[\omega_3 R (1 - \cos \theta) - \omega_3 u_r \cos \theta + \omega_3 u_\theta \sin \theta \right] \bar{a}_1 \\ & + \left[\dot{u}_r \sin \theta + \dot{u}_\theta \cos \theta \right] \bar{a}_1 + \left[\omega_3 r + \omega_3 R \sin \theta \right] \bar{a}_2 \\ & + \left[\omega_3 u_\theta \cos \theta + \dot{u}_r \cos \theta - \dot{u}_\theta \sin \theta + \omega_3 u_r \sin \theta \right] \bar{a}_2 \end{aligned} \quad (13)$$

Using Eq. (3) and Eq. (13), the partial derivative of the velocity of P with respect to the generalized speed \dot{q}_i can be obtained as:

$$\begin{aligned} \frac{\partial \bar{v}^p}{\partial \dot{q}_{1i}} = & \left[\Phi_{1j} \cos \theta \right] \bar{a}_1 - \left[\Phi_{1j} \sin \theta \right] \bar{a}_2 \\ \frac{\partial \bar{v}^p}{\partial \dot{q}_{2i}} = & \left[\Phi_{2j} \sin \theta - \frac{\cos \theta}{R} \sum_{j=1}^{\mu_2} \int_0^{\theta_0} \left(\Phi_{2j,\eta} \Phi_{2i,\eta} d\eta \right) q_{2j} \right] \bar{a}_1 \\ & + \left[\Phi_{2j} \cos \theta + \frac{\sin \theta}{R} \sum_{j=1}^{\mu_2} \int_0^{\theta_0} \left(\Phi_{2j,\eta} \Phi_{2i,\eta} d\eta \right) q_{2j} \right] \bar{a}_2 \end{aligned} \quad (14)$$

where comma denotes the partial derivative. By differentiating Eq. (13), the acceleration of P can be obtained as follows:

$$\begin{aligned} \bar{a}^p = & \left[-2\omega_3 \dot{u}_r \cos \theta + 2\omega_3 \dot{u}_\theta \sin \theta + \ddot{u}_r \sin \theta + \ddot{u}_\theta \cos \theta \right. \\ & \left. - \omega_3^2 (r + R \sin \theta) - \omega_3^2 u_r \sin \theta - \omega_3^2 u_\theta \cos \theta \right] \bar{a}_1 \\ & + \left[2\omega_3 \dot{u}_r \sin \theta + 2\omega_3 \dot{u}_\theta \cos \theta + \ddot{u}_r \cos \theta - \ddot{u}_\theta \sin \theta \right. \\ & \left. + \omega_3^2 R (1 - \cos \theta) - \omega_3^2 u_r \cos \theta + \omega_3^2 u_\theta \sin \theta \right] \bar{a}_2 \end{aligned} \quad (15)$$

By linearizing the generalized inertia forces, equa-

tions of motion can be obtained as follows.

$$\begin{aligned}
 & \sum_{j=1}^{n_1} \left[\left(\int_0^{\theta_0} R\rho\Phi_{1j}\Phi_{1j}d\theta \right) \ddot{q}_{1j} + 2\omega_3 \left(\int_0^{\theta_0} R\rho\Phi_{1j}\Phi_{2j}d\theta \right) \dot{q}_{2j} \right. \\
 & - \omega_3^2 \left(\int_0^{\theta_0} R\rho\Phi_{1j}\Phi_{1j}d\theta \right) q_{1j} + \frac{1}{R} \int_0^{\theta_0} (EA\Phi_{1j,\theta}\Phi_{1j,\theta})d\theta q_{1j} \\
 & = \omega_3^2 \int_0^{\theta_0} R\rho r \cos\theta\Phi_{1j}d\theta + \omega_3^2 \int_0^{\theta_0} R^2\rho \sin\theta\Phi_{1j}d\theta \\
 & \sum_{j=1}^{n_2} \left[\left(\int_0^{\theta_0} R\rho\Phi_{2j}\Phi_{2j}d\theta \right) \ddot{q}_{2j} - 2\omega_3 \left(\int_0^{\theta_0} R\rho\Phi_{2j}\Phi_{1j}d\theta \right) \dot{q}_{1j} \right. \\
 & - \omega_3^2 \left(\int_0^{\theta_0} R\rho\Phi_{2j}\Phi_{2j}d\theta \right) q_{2j} + \frac{1}{R^3} \int_0^{\theta_0} (E\mathbf{K}_{2j,\theta\theta}\Phi_{2j,\theta\theta})d\theta q_{2j} \\
 & + \frac{1}{R^3} \left(\int_0^{\theta_0} E\mathbf{K}_{2j,\theta\theta}\Phi_{2j}d\theta + E\mathbf{K}_{2j,\theta\theta}\Phi_{2j}d\theta + E\mathbf{K}_{2j}\Phi_{2j}d\theta \right) q_{2j} \\
 & - \omega_3^2 r\rho \left\{ \int_0^{\theta_0} (\sin\theta - \sin\theta_0)\Phi_{2j,\theta}\Phi_{2j,\theta}d\theta \right\} q_{2j} \\
 & + \omega_3^2 r\rho \left\{ \int_0^{\theta_0} (\cos\theta - \cos\theta_0)\Phi_{2j,\theta}\Phi_{2j,\theta}d\theta \right\} q_{2j} \Big] \\
 & = \omega_3^2 \int_0^{\theta_0} R\rho r \sin\theta\Phi_{2j}d\theta - \omega_3^2 \int_0^{\theta_0} R^2\rho \cos\theta\Phi_{2j}d\theta \\
 & + \omega_3^2 \int_0^{\theta_0} R^2\rho\Phi_{2j}d\theta
 \end{aligned} \tag{16}$$

The underlined terms in Eq. (17) indicate the stiffness variations induced by rotational motion.

2.4 Dimensionless equations of motion

To lend generality to the numerical results, Eqs. (16, 17) need to be transformed into dimensionless equations. Several dimensionless variables and parameters can be defined as follows:

$$\tau = \frac{t}{T} \tag{18}$$

$$\xi = \frac{\theta}{\theta_0} \tag{19}$$

$$\bar{q}_j = \frac{q_j}{R\theta_0} \tag{20}$$

$$\delta = \frac{r}{R} \tag{21}$$

$$\gamma = T\omega_3 \tag{22}$$

where

$$T = \sqrt{\frac{\rho R^4 \theta_0^4}{EI}} \tag{23}$$

The parameters γ and δ represent the angular speed ratio and the hub radius ratio. The right hand side terms of the equations of motion, which only result in forced responses of the system, can be ig-

nored for the modal analysis. So,

$$\sum_{j=1}^{n_1} [m_{ij}^{11} \ddot{\bar{q}}_{1j} + 2\gamma m_{ij}^{12} \dot{\bar{q}}_{2j} - \gamma^2 m_{ij}^{11} \bar{q}_{1j} + \alpha^2 k_{ij}^S \bar{q}_{1j}] = 0 \tag{24}$$

$$\sum_{j=1}^{n_2} [m_{ij}^{22} \ddot{\bar{q}}_{2j} - 2\gamma m_{ij}^{21} \dot{\bar{q}}_{1j} - \gamma^2 m_{ij}^{22} \bar{q}_{2j} + k_{ij}^B \bar{q}_{2j} + \gamma^2 \delta k_{ij}^{GC} \bar{q}_{2j} + \gamma^2 k_{ij}^{GS} \bar{q}_{2j}] = 0 \tag{25}$$

where α , which is often called the slenderness ratio, is defined as

$$\alpha = \left(\frac{A(R\theta_0)^2}{I} \right)^{1/2} \tag{26}$$

and

$$m_{ij}^{\alpha\beta} = \int \psi_{\alpha i} \psi_{\beta j} d\xi \tag{27}$$

$$k_{ij}^S = \int \psi_{1j,\xi} \psi_{1i,\xi} d\xi \tag{28}$$

$$k_{ij}^B = \int \psi_{2j,\xi} \psi_{2i,\xi} d\xi + \theta_0^2 \int \psi_{2j,\xi} \psi_{2i,\xi} d\xi + \theta_0^2 \int \psi_{2j,\xi} \psi_{2i,\xi} d\xi + \theta_0^2 \int \psi_{2j} \psi_{2i} d\xi \tag{29}$$

$$k_{ij}^{GC} = \frac{1}{\theta_0} \int \cos \frac{(\xi+1)\theta_0}{2} \sin \frac{(1-\xi)\theta_0}{2} \psi_{2j,\xi} \psi_{2i,\xi} d\xi \tag{30}$$

$$k_{ij}^{GS} = \frac{1}{\theta_0} \int \sin \frac{(\xi+1)\theta_0}{2} \sin \frac{(1-\xi)\theta_0}{2} \psi_{2j,\xi} \psi_{2i,\xi} d\xi \tag{31}$$

In Eqs. (27-31), $\psi_{\alpha i}$ denotes a function of ξ which produces the same value as $\phi_{\alpha i}$.

2.5 Modal formulation

Eq. (24) and Eq. (25) are expressed in a matrix form as

$$\begin{bmatrix} M_{11} & 0 \\ 0 & M_{22} \end{bmatrix} \begin{Bmatrix} \ddot{\bar{q}}_{1j} \\ \ddot{\bar{q}}_{2j} \end{Bmatrix} + \begin{bmatrix} 0 & C_{12} \\ C_{21} & 0 \end{bmatrix} \begin{Bmatrix} \dot{\bar{q}}_{1j} \\ \dot{\bar{q}}_{2j} \end{Bmatrix} + \begin{bmatrix} K_{11} & 0 \\ 0 & K_{22} \end{bmatrix} \begin{Bmatrix} \bar{q}_{1j} \\ \bar{q}_{2j} \end{Bmatrix} = 0 \tag{32}$$

In Eq. (32), M_{11} and M_{22} denote matrices which are composed of elements m_{ij}^{11} and m_{ij}^{22} . The other sub-matrices are defined as follows:

$$C_{12} = -2\gamma M_{12} \tag{33}$$

$$C_{21} = +2\gamma M_{21} \tag{34}$$

$$K_{11} = -\gamma^2 M_{11} + \alpha^2 K_S \tag{35}$$

$$K_{22} = -\gamma^2 M_{22} + K_B + \gamma^2 \delta K_{GC} + \gamma^2 K_{GS} \tag{36}$$

where the elements of K_S , K_B , K_{GC} , and K_{GS} are given in Eqs. (28-31).

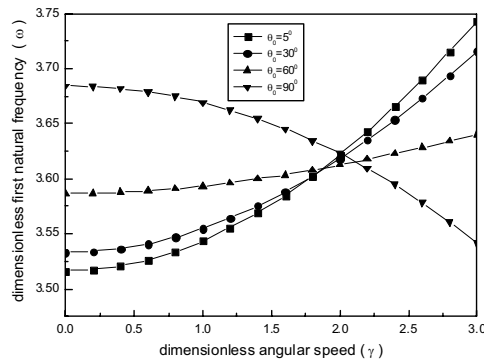
3. Numerical study and discussion

In Table 1, the first dimensionless natural fre-

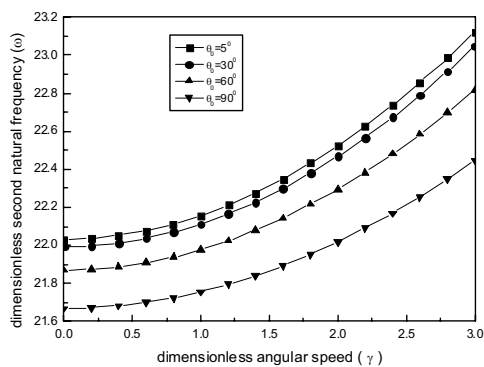
quency of the non-rotating cantilevered curved beams obtained with the present modeling method is compared to those of Ref. [12] in which the Rayleigh-Ritz method is employed to obtain the upper bound and

Table 1. Comparison of the first dimensionless natural frequency ($\alpha = 70$).

θ_0 (degree)	Upper bound Ref. [12]	Lower bound Ref. [12]	Present
10	3.51	3.47	3.52
20	3.52	3.47	3.52
30	3.53	3.48	3.53
40	3.55	3.50	3.55
50	3.57	3.52	3.56
60	3.59	3.54	3.59
70	3.62	3.57	3.61
80	3.66	3.60	3.65
90	3.71	3.64	3.68



(a)



(b)

Fig. 2 Variations of dimensionless natural frequencies (a) the first frequency (b) the second frequency (δ used to obtain the above results is 0).

Dunkerley’s method is employed to obtain the lower bound. This shows that the present method is qualitatively equivalent to the conventional modeling method if the motion induced stiffness variation effects are ignored.

The natural frequencies of straight beams increase as the rotating speed increases. For curved beams with large radius and small arc angle (almost straight beam), their natural frequencies increase as those of straight beams do. However, when the arc angle gets larger, the first natural frequency may decrease rather than increase.

Fig. 2 shows the dimensionless natural frequencies ω which can be obtained by multiplying the natural frequencies by T as defined in Eq. (24). To obtain the results, eight assumed modes are used. When the arc angle remains small, the first frequency increases as shown in Fig. 2(a). But as the arc angle increases, the increasing rate of the first frequency attenuates. The variation of second natural frequency is shown in Fig. 2(b). It exhibits only increasing trends as that of the straight beam. As the angular speed increases, the second natural frequency increases. When the arc angle increases, the second natural frequency locus shifts to the lower direction.

If the angular speed of the rotating beam matches the natural frequency (as shown in Fig. 3(a)), the angular speed is called the tuned angular speed. Severe resonance phenomena may occur at the tuned angular speed. So the tuned angular speed must be calculated for the safe design of a rotating beam. The tuned angular speeds for three different hub radius ratios and four curvature angles are shown in Fig. 3.

The above figures indicate that the arc angle of the circular arc beam may significantly affect the location of the tuned angular speed. The case of zero hub radius ratio is shown in Fig. 3(a). It is observed that the tuned angular speed varies with the arc angle. As the arc angle increases, the tuned angular speed decreases. Fig. 3(b) indicates that the beam with an arc angle less than a certain value may have no tuned angular speed if the hub radius ratio exceeds a certain value. Fig. 3(c) shows that the tuned angular speed exists only if the arc angle becomes large enough. As the hub radius ratio increases, the tuned angular speed of a beam with a certain arc angle increases. Also the tuned angular speed of a beam with small arc angle disappears when the hub radius ratio increases.

The lowest four natural frequency loci for two arc angles are plotted in Fig. 4. The solid lines represent

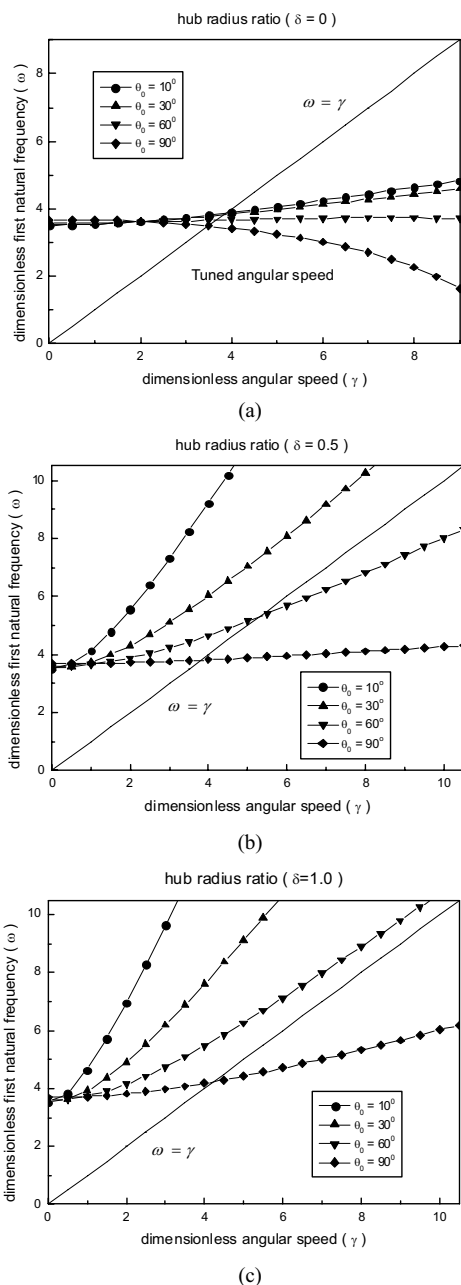


Fig. 3. Variation of the first dimensionless natural frequency for three hub radius ratios and four arc angles (a) $\delta = 0$ (b) $\delta = 0.5$ (c) $\delta = 1$.

the results with the coupling effect considered, and the dotted lines represent the results with the coupling effect ignored (C_{12} and C_{21} are assumed 0 in Eq. (32)). Dimensionless variables of $\delta = 0.1$ and $\alpha = 70$ are used to obtain the results. When $\alpha = 70$, the beam is slender enough to satisfy the Eulerian

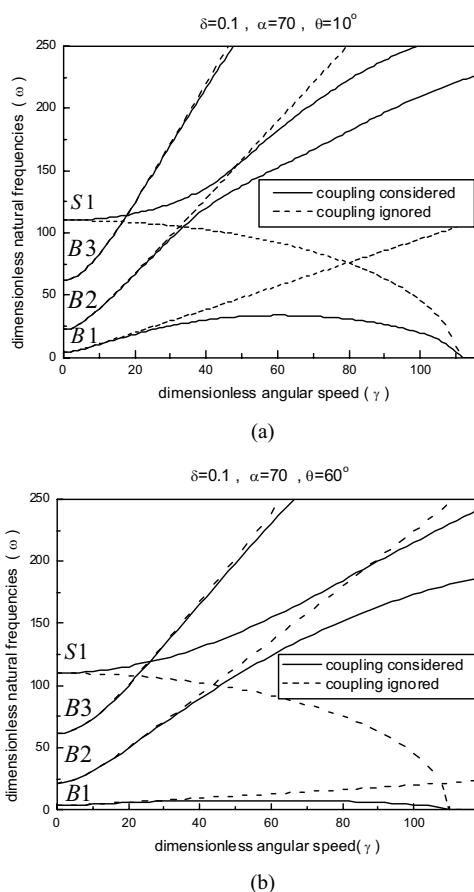


Fig. 4. Variations of the natural frequencies for two arc angles with or without the coupling effect (a) $\theta_0 = 10^\circ$ (b) $\theta_0 = 60^\circ$.

beam assumption. At $\gamma = 0$, the first three of the loci represent the lowest three bending frequencies and the fourth represents the first stretching natural frequency. The trend of the results coincides with that of Ref. [5]. The comparisons of coupling effect with arc angles of 10° and 60° are shown in Fig. 4(a) and Fig. 4(b). These results indicate that the arc angle mainly affects the first bending natural frequency when the coupling effect is considered.

In Fig. 5, the first bending natural frequency loci with three different arc angles are shown. This figure shows that there exists an angular speed where the first bending natural frequency becomes zero. The rotating cantilevered beam will buckle when the natural frequency becomes 0. So the angular speed will be called the buckling speed. It indicates that as the arc angle increases, the buckling speed decreases. When the arc angle increases, the difference between the

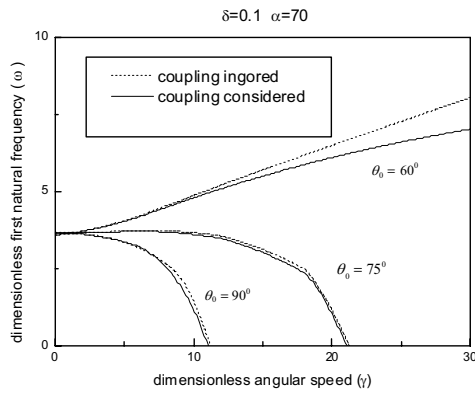


Fig. 5. Variation of the first bending natural frequency with three different arc angles.

coupling considered result and the coupling ignored result becomes negligible. As the arc angle remains small, the loci become similar to those of a straight beam. Fig. 5 shows that the buckling speed decreases and the coupling effect becomes negligible as the arc angle increases.

4. Conclusions

In this study, the equations of motion of rotating cantilevered circular arc beams are derived by using a modeling method that employs a stretch variable. The equations are transformed into dimensionless forms in which dimensionless parameters are identified. The natural frequencies versus the rotating angular speed are numerically obtained. The slenderness ratio used for the numerical simulation is 70 and the limit of the arc angle is 90° . While the first natural frequency of a straight cantilevered beam increases as the rotating angular speed increases, that of a circular arc beam decreases if the arc angle exceeds a certain value. If the hub radius ratio exceeds a certain value, the tuned angular speed, where the angular motion frequency is equal to the first natural frequency, does not exist. The equations governing bending motion are coupled with those governing stretching motion. When the coupling effect is considered, a buckling speed can be obtained effectively. It was shown that the coupling effect becomes negligible as the arc angle increases.

Acknowledgments

This research was supported by the Center of Innovative Design Optimization Technology (iDOT), Korea Science and Engineering Foundation.

References

- [1] Southwell and Gough, The free transverse vibration of airscrew blades, British A.R.C. Report and Memoranda 766 (1921).
- [2] M. Schilhansl, Bending frequency of a rotating cantilever beam, *J. Applied Mechanics*. 25 (1958) 28-30.
- [3] S. Putter and H. Manor, Natural frequencies of radial rotating beams, *J. Sound and Vibration*. 56 (1978) 175-185.
- [4] T. Kane, R. Ryan, and A. Banerjee, Dynamics of a cantilever beam attached to a moving base, *J. Guidance, Control, and Dynamics*. 10 (2) (1987) 139-151.
- [5] H. Yoo and S. Shin, Vibration analysis of rotating cantilevered beams, *J. Sound and Vibration*. 212 (5) (1998) 807-828.
- [6] A. Love, A Treatise on the Mathematical Theory of Elasticity, 4th ed, Dover, New York, (1944) 444-454.
- [7] S. Lee and J. Chao, Exact out-of-plane vibration for curved non-uniform beams, *J. Applied Mechanics*. 68 (2001) 181-191.
- [8] R. Hoppe, The bending vibration of a circular ring, *J. Mathematics*. 73 (1971) 158.
- [9] S. Timoshenko, Vibration Problems in Engineering, John Wiley & Sons, Inc (1974).
- [10] L. Plilipson, On the role of extension in the flexural vibration of rings, *J. Applied Mechanics*. 23 (1956) 364-366.
- [11] P. Laura, In-plane vibration of an elastically cantilevered circular arc with a tip mass, *J. Sound and Vibration*. 115 (1987) 37-466.
- [12] M. Petyt and C. Fleishe, Free vibration of a curved beam, *J. Sound and Vibration*. 18 (1971) 17-30.
- [13] T. Kane and D. Levinson, Dynamics: Theory and Application, McGraw-Hill, New York (1995).
- [14] L. Eisenhart, An Introduction to Differential Geometry, Princeton University Press, (1947).